International Journal of Science and Research Archive

eISSN: 2582-8185

Cross Ref DOI: 10.30574/ijsra

Journal homepage: https://ijsra.net/

(RESEARCH ARTICLE)

Simulation study on the effect of intake charge temperature and ignition timing on the performance of a converted biogas engine

Nguyen Thanh Cong [1], Nguyen Phi Truong [2, *], Vu Ngoc Quynh [3], Dong Duc Huy [3], Nguyen Ngoc Anh [3] and Vu Minh Dien [3]

[1] *Faculty of Mechanical Engineering, University of Transport and Communications, 3 Cau Giay, Hanoi, Vietnam.*
[2] *Faculty of Transportation Engineering, School of Mechanical and Automotive Engineering, Hanoi University of Industry, Minh Khai Ward, Bac Tu Liem District, Hanoi, Vietnam.*
[3] *Department of Automobile Technology, Center for Automotive Technology and Driver Training, Hanoi University of Industry, Minh Khai Ward, Bac Tu Liem District, Hanoi, Vietnam.*

International Journal of Science and Research Archive, 2025, 15(02), 744-757

Publication history: Received on 29 March 2025; revised on 10 May 2025; accepted on 12 May 2025

Article DOI: https://doi.org/10.30574/ijsra.2025.15.2.1354

Abstract

This study conducts a simulation analysis of the performance and emission characteristics of a biogas-fueled engine using the thermodynamic simulation tool AVL Boost. The original diesel engine model was modified by lowering the compression ratio and enhancing mixture formation to enable operation with biogas. Key engine parameters such as airflow mass, brake torque and power, fuel consumption, emission outputs, and in-cylinder parameters were evaluated. The simulation results indicate that, under biogas operation, NOx emissions decrease significantly, while CO emissions rise compared to diesel-fueled operation. Although the engine's brake power shows a decline when fueled by biogas, fuel efficiency demonstrates an improvement trend. Additionally, the impact of ignition timing and charge temperature on engine behavior was examined. Findings suggest that the optimal ignition timing for biogas engines should be set between 11° and 19° crank angle before top dead center. The intake charge temperature affects the combustion process and the engine's output power. Ideally, the intake air temperature should be maintained below 50°C to ensure optimal engine performance and technical reliability.

Keywords: Biogas; AVL Boost; Emission; Compression ratio; In-cylinder parameters

1. Introduction

Numerous studies have confirmed that curbing air pollution from road vehicles remains a major concern for developing countries. As a result, researchers have shifted their attention toward finding alternatives to traditional fossil fuels. In Vietnam, both modern and older vehicles have been experimented with using alternative fuels. Various options like biodiesel [1], liquefied petroleum gas (LPG) [2], natural gas (NG) [3], and biogas [4] have seen notable development through extensive research efforts.

Natural gas, primarily composed of methane (CH_4), is among the potential candidates for replacing conventional fuels in internal combustion engines. Utilizing gaseous fuels can contribute to lowering emissions of NO_x, particulate matter, and greenhouse gases from diesel engines [5]. Thanks to CH_4's higher hydrogen-to-carbon ratio compared to gasoline [6], emissions of carbon monoxide (CO) and carbon dioxide (CO_2) can also be reduced. Additionally, biogas fosters more homogeneous air-fuel mixtures, promoting better combustion and subsequently lowering hydrocarbon (HC) emissions. Gas engines, particularly during cold starts, emit fewer hydrocarbons than petrol engines because there is less absorption and desorption of fuel by the lubricating oil and cylinder walls [7].

* Corresponding author: Nguyen Phi Truong.

Biogas presents two main utilization pathways: it can either be used directly in spark-ignition (S.I.) engines or serve as a supplementary fuel in diesel engines under dual-fuel configurations. Nevertheless, its slow combustion speed and high RON (Research Octane Number) can prolong combustion duration and slightly diminish thermal efficiency [8]. Researchers have observed that petrol engines converted to operate on NG often suffer from performance drawbacks despite improved emissions quality. Adding NG decreases the mass of intake air, reducing overall engine output. Yontar and Doğu (2018) reported a 10% decrease in volumetric efficiency when pure CH_4 was used in dual-fuel NG-gasoline S.I. engines [9]. Furthermore, mixing CH_4 with external gasoline, even with optimized ignition timing (IT), led to a 16% drop in brake mean effective pressure (BMEP) [10]. Biogas, due to its relatively low heating value of approximately 23,400 kJ/m^3 [9], further contributes to reduced engine performance. Surata et al. (2014) [11] explored the use of biogas in a generator powered by an S.I. engine, revealing that although no extensive modifications to the engine itself were necessary, the carburetor had to be replaced with a specialized mixer. When using a mixer to operate with gaseous fuels, the engine's effective power decreased in comparison to the original engine configuration. Another study highlighted that optimizing an S.I. engine for biogas required increasing the compression ratio from 8.5:1 to 9:1 to achieve acceptable performance levels [12].

In dual-fuel operation, where biogas complements diesel fuel, Barik and Murugan [13] demonstrated improvements in engine efficiency and a decrease in diesel consumption. To maximize performance, it was necessary to advance the diesel injection timing from 23° to 26° before top dead center (TDC). However, this mode of operation also led to increases in HC and CO emissions by 2% and 10%, respectively, relative to standard diesel usage. On the other hand, smoke emissions dropped by around 39%, and nitrogen oxide (NO_x) emissions decreased by 16%. Despite these emission benefits, the brake-specific fuel consumption (BSFC) rose by approximately 25% under full-load conditions compared to diesel-only operation. For diesel engines to operate exclusively on biogas, conversion to a S.I. system is required. According to findings from Omnitek [14], turbocharged diesel engines can be adapted for pure biogas operation by implementing several modifications, such as replacing the diesel injection system with a S.I. system, reducing the compression ratio, adjusting the boost pressure, and integrating an appropriate air-fuel mixing system.

In Vietnam, incorporating gaseous fuel into the transportation sector presents a viable strategy for reducing reliance on fossil fuels and lowering emissions, thereby supporting the nation's sustainability objectives. Nevertheless, research on converted engines operating exclusively on gas fuel or biogas remains relatively scarce. Some studies have investigated biogas engines [15], but further research is necessary to expand biogas application in the automotive field. As discussed earlier, several technical challenges must be addressed when using pure gas fuel, including compression ratio reduction, ignition timing adjustments, intake air temperature control, and the use of appropriate fuel additives [16]. In this context, the research team employs simulation techniques to optimize operating parameters and propose viable solutions for adapting converted engines to run fully on biogas.

This study focuses on overcoming the barriers associated with biogas fueled by evaluating technical performance and emission behavior in a converted engine. Originally equipped with a port fuel injection system, the vehicle was modified for ethanol compatibility. Furthermore, AVL-Boost simulation software was applied to investigate critical combustion parameters such as in-cylinder pressure, providing a deeper understanding of biogas combustion characteristics and engine performance.

2. Material and methodology

2.1. Study procedure

The research procedure follows several stages, as shown in Figure 1. Initially, the simulation model is constructed using technical specifications and actual engine structural data. Following this, the model's accuracy is validated by comparing selected simulation outcomes with corresponding experimental results. Once the model demonstrates satisfactory accuracy, the model was modified to operate with biogas fuel by adjusting structural parameters and the type of fuel used. The economic and performance characteristics of the ethanol-fueled engine are subsequently evaluated based on the established simulation scenarios.

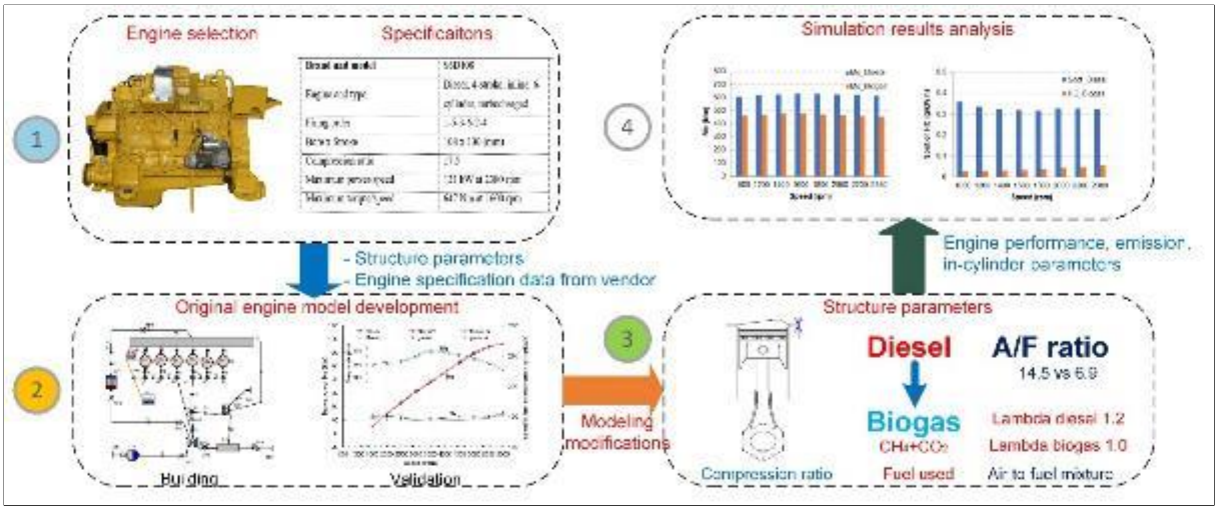

Figure 1 The study procedure flowchart

2.2. Basis for converting diesel engines to biogas engines

To utilize biogas as a fuel for internal combustion engines, the engine's compression ratio typically needs to be lower than 16:1 to prevent knocking [17]. However, for turbocharged engines, an even lower compression ratio is required for the conversion. Methods to reduce the compression ratio include modifying the piston crown or increasing the thickness of the cylinder head gasket. If the piston crown is precisely machined at appropriate locations, it can enhance swirl motion within the combustion chamber, promoting better air-fuel mixture formation and improving combustion quality. However, machining the piston crown alters the piston's mass and its durability [18], potentially affecting the engine's dynamics.

Increasing the cylinder head gasket thickness offers several advantages: it minimally impacts other mechanical structures of the engine, requires less modification work, and is cost-effective. However, the shape of the piston crown and the combustion chamber volume at top dead center are not fully compatible with biogas fuel. Nonetheless, when increasing the gasket thickness, it is essential to ensure proper sealing to prevent lubricating oil and coolant leakage, which could damage the engine.

In this study, the optimal approach chosen for reducing the compression ratio is to increase the cylinder head gasket thickness, while maintaining the original combustion chamber shape. The additional gasket thickness depends solely on the piston stroke, as well as the original and target compression ratios. The required increase in gasket thickness is determined according to Equation (1).

$$a = S.\frac{\varepsilon - \varepsilon_0}{(\varepsilon-1)(\varepsilon_0-1)} \qquad \ldots\ldots\ldots \quad (1)$$

Where, ε and ε_0 represent the compression ratios before and after the modification, respectively, S denotes the piston stroke (mm), and a refers to the thickness of the spacer to be added (mm).

2.3. Simulation fuel

Table 1 presents a comparison of the fuel properties. The referenced characteristics are sourced from the literature [19, 20], while the biogas composition data were derived from practical applications.

Table 1 Main characteristics of fuels [19, 20]

Properties	Diesel	Biogas
Composition	$C_xH_yO_z$	CH_4-65%, CO_2-34.2%, CO-0.26%, H_2-0.10%, and traces of other gases (measured data on test site at pig farm)
Lower heating value (LHV) (MJ/kg)	42,5	23,6
Density (kg/m^3)	825 (liquid)	1.21 (gas)
Flame speed (m/s)	0.3	0.25
Stoichiometric air-to-fuel ratio (kg in air/kg in fuel)	14.5	≈ 6.05
Cetane number	55	-
RON	-	130
Auto ignition temperature (k)	553	923
Flammability limit (% vol)	0.7-5	7.5-14

2.4. Simulation model development

The experimental research in this study was conducted on a widely used vehicle, with the primary engine specifications detailed in Table 2.

Table 2 The test engine specifications

Brand and model	S6D108
Engine and type	Diesel, 4-stroke, inline, 6-cylinder, turbocharged
Firing order	1-5-3-6-2-4
Bore x Stroke	108 x 130 (mm)
Compression ratio	17.5
Maximum power/speed	121 kW at 2380 rpm
Maximum torque/speed	647 Nm at 1600 rpm

According to the results from simulation and experimental studies on the effect of compression ratio on the performance of biogas engines [17], the optimal compression ratio for a biogas engine falls within the range of 11.5 to 12.5. In this study, the compression ratio after modification was selected to be 12.5. Therefore, based on Equation (1), the additional thickness of the gasket required is determined as follows:

$$a = S \times \frac{\varepsilon - \varepsilon_o}{(\varepsilon - 1)\times(\varepsilon_o - 1)} = 130 \times \frac{17.5 - 12.5}{(17.5-1)\times(12.5-1)} = 3.43\ mm \qquad \ldots\ldots\ldots \quad (2)$$

When direct measurement methods are not feasible or experimental setups become overly complicated for analyzing specific parameters, simulation modeling offers a viable alternative. In this research, AVL Boost commercial software was utilized to construct a simulation model aimed at predicting the effects of different fuels and technical modifications on the combustion process, in-cylinder dynamics, and overall engine performance, while minimizing experimental costs.

The developed model, depicted in Figure 2, was structured based on the engine's geometric and design parameters. The simulation relies on the first law of thermodynamics to calculate the engine's pressure cycle. The AVL MCC combustion model was applied to simulate the combustion process in the diesel engine. This model is capable of predicting the heat release rate as well as key in-cylinder parameters, including pressure, temperature, and the formation of emissions such as NO_x, CO, and soot [21]. For S.I. engines, the Fractal combustion model was employed to investigate the combustion process and estimate the heat release rate, particularly for engines characterized by extended mixing times or homogeneous mixtures. The Fractal model also allows prediction of NO_x, CO, and HC emissions, in addition to combustion parameters like ignition delay and the octane number required for the fuel [22].

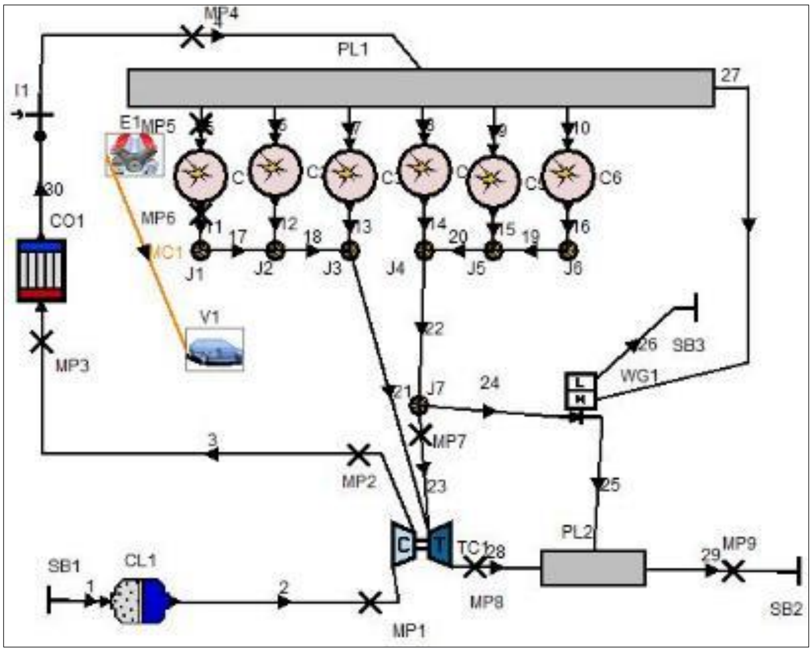

Figure 2 The developed model of the engine in AVL Boost

To compare the changes in technical performance when transitioning from diesel to biogas, two models were simulated under full load conditions. In the biogas engine simulations, the air-fuel equivalence ratio was maintained at the stoichiometric value of 1.0, whereas for the diesel engine, the air excess ratio was set at 1.2 (concerning full load condition). Regarding fuel properties used in modeling, diesel characteristics were sourced from the default chemical-thermal database provided by AVL. The main differences between the two models are illustrated in Figure 3.

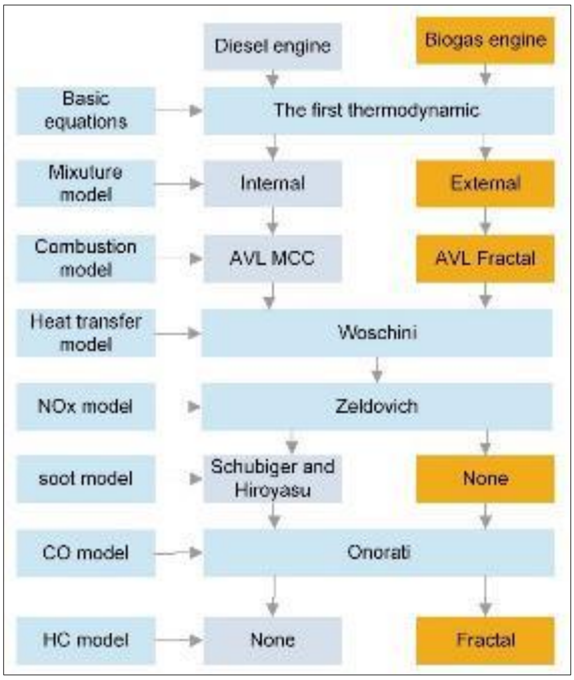

Figure 3 Comparison of basic theory and models of diesel and biogas simulation models

2.5. Simulation scenario

First, the model was run using diesel under full load conditions as a baseline to evaluate the model's reliability by comparing power output, torque, and fuel consumption data between the simulation results and the manufacturer's specifications. Once the model demonstrated acceptable accuracy, with deviations in specific fuel consumption and power/torque output being less than 5%, gasoline was modified to S.I. engine and fueled with biogas fuel.

The simulation results for biogas were compared with the original diesel engine to highlight the benefits of using biogas and the changes in engine performance. Additionally, two other operating parameters, including ignition timing and intake air temperature, were investigated. The intake air temperature was varied from 25°C to 75°C, while the ignition timing was adjusted from 5 degrees to 21 degrees before top dead center (TDC).

3. Results and discussion

3.1. Validation of simulation models

Figure 4 presents the indicated mean effective pressure (IMEP) and brake mean effective pressure (BMEP) values across simulated cycles under rated operation at 1600 rpm at an air excess ratio of 1.2. It can be seen that both the IMEP and BMEP graphs share a similar overall trend: the initial values fluctuate significantly during the first few cycles, then quickly decrease to a stable value of 15,03 bar for IMEP and 13.64 bar for BMEP. This confirms that the simulation data have converged, making them suitable for further comparative studies.

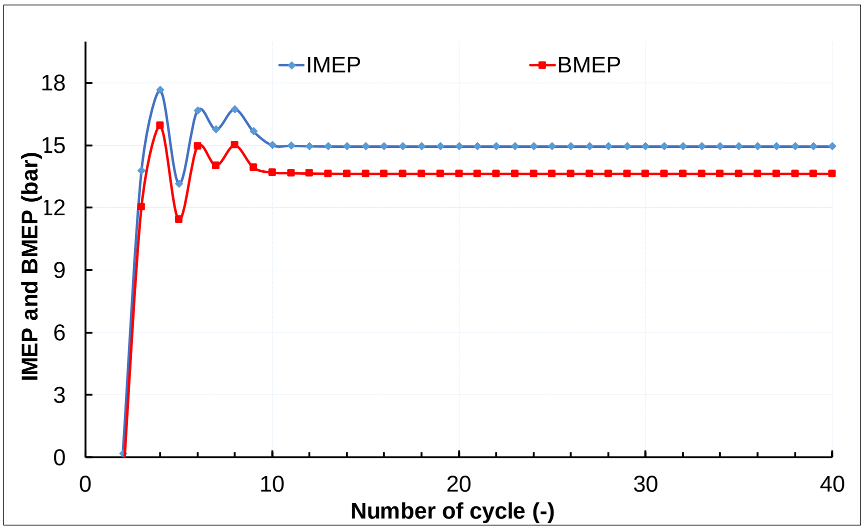

Figure 4 The simulated IMEP and BMEP as a function of cycles at an air excess ratio of 1.2 and an engine speed of 1600 rpm

To ensure accuracy, the simulation model was validated by comparing its outcomes with data supplied by the vendor under varying engine operating conditions, as shown in Figure 5. The results indicate that the trends in brake power and torque from the simulation closely match those observed in the experiment at full load for the same input energy. This demonstrates strong consistency between both datasets. The difference between simulated and experimental brake power and torque values averaged deviation is 4.20% and 5.15% across the entire simulated speed range. Minor discrepancies arise due to certain assumptions made in the simulation that cannot be precisely controlled in practical tests. However, these variations are minimal, confirming the reliability of the simulation model for further combustion studies.

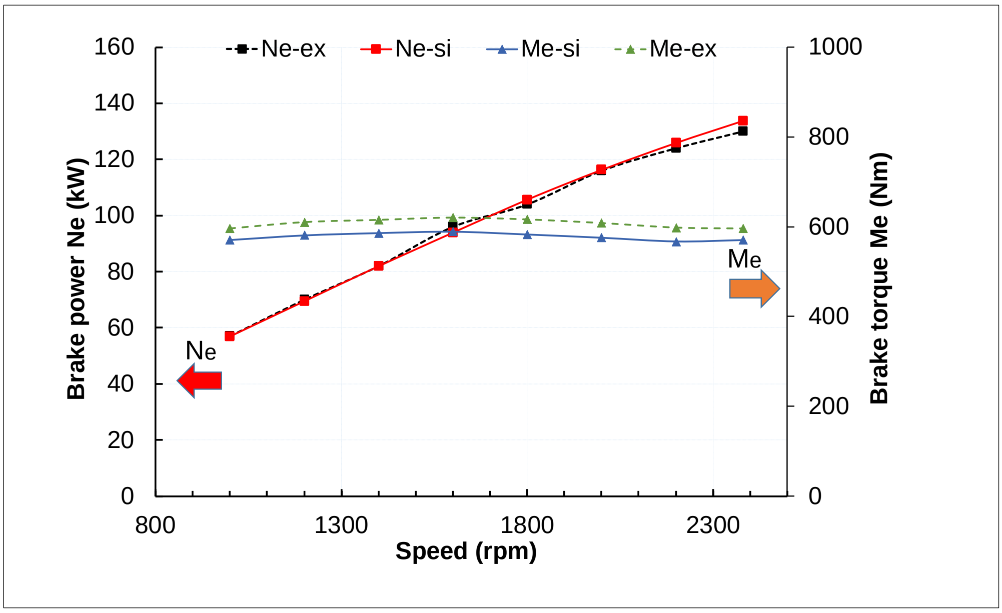

Figure 5 Comparison of brake power and torque at full load conditions

3.2. The engine performance comparison of biogas and the original diesel engine

From the simulation results, values for intake airflow rate, engine power, torque, fuel consumption, in-cylinder pressure and temperature, and harmful emissions were determined for the engine operating on biogas fuel, and compared to those using diesel fuel under full throttle conditions across various engine speeds. Figures 6 and 7 illustrate the engine torque and power under load conditions from 1000 rpm to 2380 rpm for both diesel and biogas fuels. Across the entire speed range, engine power (N_e) and torque (M_e) decreased by approximately 24% to 27% when operating with biogas compared to diesel. When comparing fuel economy performance, since biogas has a significantly lower calorific value than diesel, the comparison should be based on the brake specific energy consumption (BSEC), which is determined using the following equation:

$$BSEC = \frac{m \times LHV}{Ne} \qquad \text{..........} \qquad (3)$$

Where: m is mass of fuel, LHV is the lower heating value of fuel, and N_e is brake power.

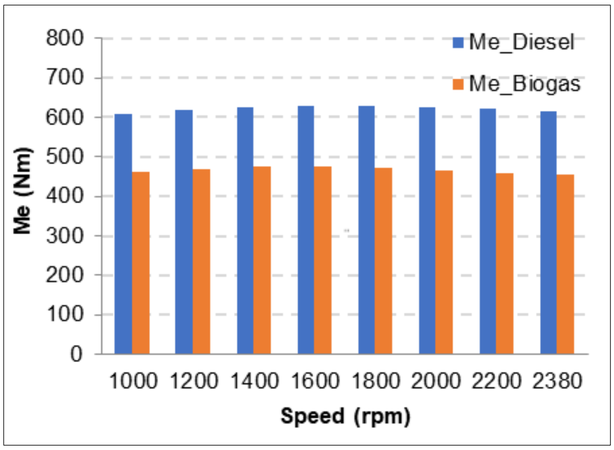

Figure 6 Brake torque comparison

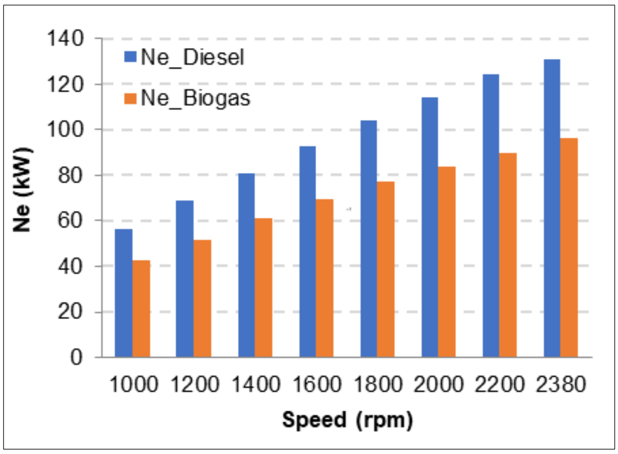

Figure 7 Brake power comparison

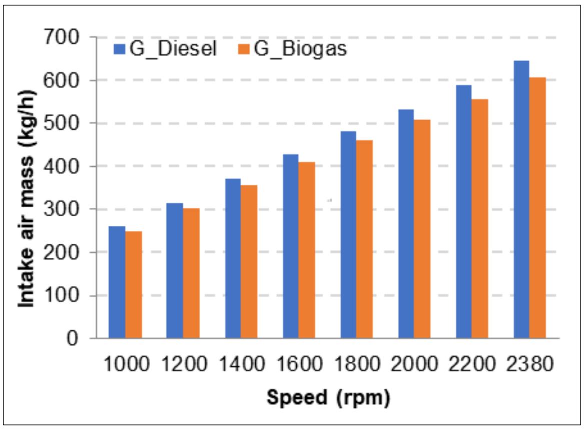

Figure 8 Intake air mass comparison

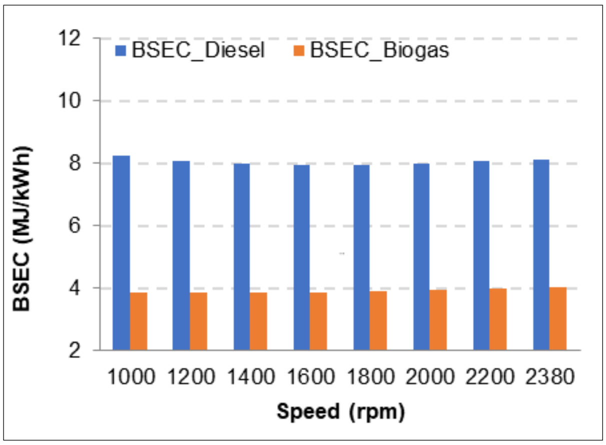

Figure 9 Brake-specific energy consumption comparison

The reduction in power and torque is attributed to the large volume of biogas introduced into the intake manifold, which displaces intake air, thereby decreasing the mass of air entering the cylinder and subsequently reducing engine power and torque. Figure 8 shows the intake airflow rate of the engine across different speeds for both diesel and biogas fuels. On average, the intake airflow rate decreases by approximately 4.59% when using biogas compared to diesel. The results presented in Figure 9 indicate that the engine's specific fuel consumption is improved when operating on biogas compared to diesel, with an average reduction of about 51.48%.

3.3. The engine pollutants comparison of biogas and the original diesel engine

Figures 10 to 12 illustrate the harmful pollutants of soot, HC, CO, and NO_x from the engine operating under full-load conditions across engine speeds ranging from 1000 rpm to 2380 rpm, using both diesel and biogas fuels. Figure 10 shows that when operating on biogas, soot emissions are eliminated, but HC emissions are generated due to the difference in the combustion model in AVL-Boost. In practice, diesel engines emit very low levels of HC, while S.I. engines virtually do not produce black smoke emissions. Soot is typically formed under conditions of low excess air and high temperatures, where acetylene compounds are produced from the decomposition of long-chain alkanes in diesel fuel within fuel-rich environments [23]. HC emissions arise from the formation of air-fuel mixtures outside the cylinder and result from incomplete combustion processes. In addition, HC can also be produced during the overlap phase [24]. Although HC emissions are generated when using biogas, soot emissions are completely eliminated, and the average amount of HC emissions is only about 12% of the soot under diesel operation.

The results presented in Figure 11 show that the engine's CO emissions are higher when operating on biogas compared to diesel fuel, with an average increase of 97% and an average rise of 68 ppm in CO concentration. This increase is attributed to numerous lean mixture zones resulting in incomplete combustion processes, which collectively lead to elevated CO emissions. The results shown in Figure 12 indicate that the engine's NO_x emissions decrease significantly when operating on biogas compared to diesel fuel, with an average reduction of 1270 ppm, equivalent to 99%. The primary reason for the reduction in NO_x emissions is the lower peak combustion temperature, which is clearly demonstrated in the simulated in-cylinder pressure and temperature results (Figures 13 and 14).

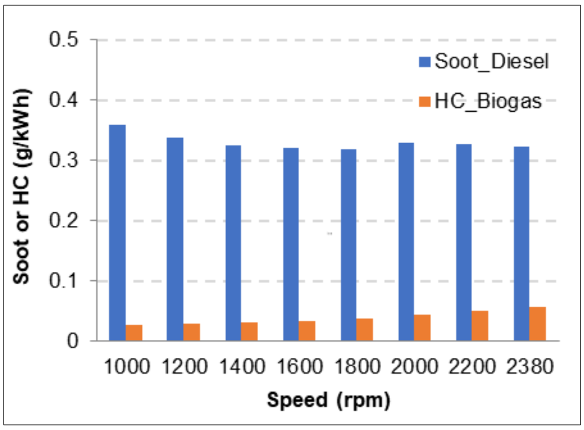

Figure 10 Comparison of soot and HC

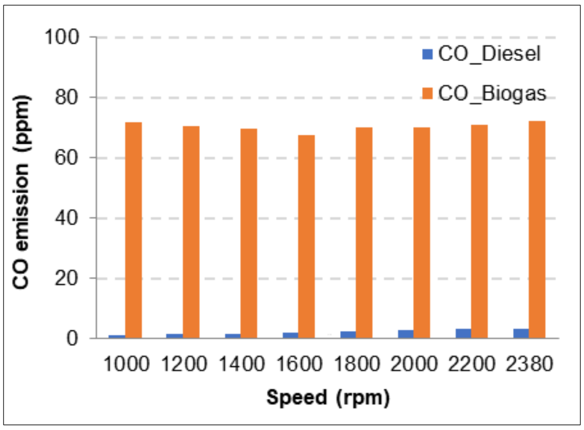

Figure 11 Comparison of CO

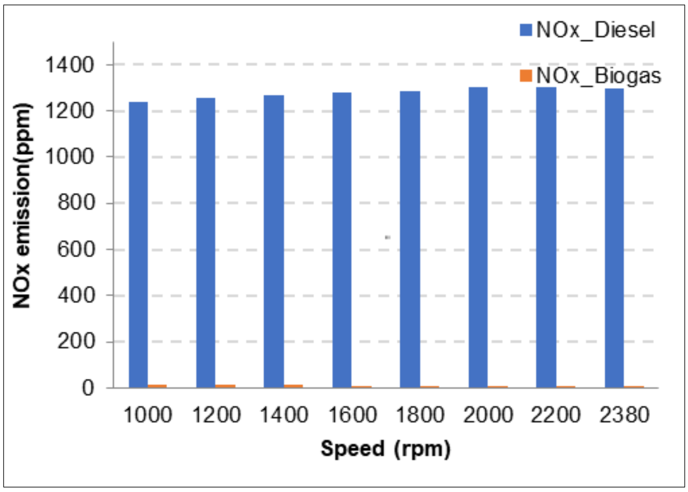

Figure 12 Comparison of NO_x

3.4. The in-cylinder pressure and temperature comparison of biogas and the original diesel engine

Figure 13 shows that the in-cylinder pressure for biogas combustion is lower than that for diesel. The peak pressure when using diesel reaches 99 bar at a crank angle of 366°, whereas for biogas it is 46 bar at 380° crank angle. Similarly, Figure 14 illustrates that the in-cylinder combustion temperature when using biogas is also lower than that for diesel at the default IT of the diesel engine of 17°. The peak temperature for diesel combustion is 2155 K at 380° crank angle, while for biogas it is 1917 K at 394° crank angle. It can be observed that when operating with biogas, not only are the peak pressure and temperature reduced, but the combustion process is also delayed, shifting further to the right on the graph compared to diesel operation.

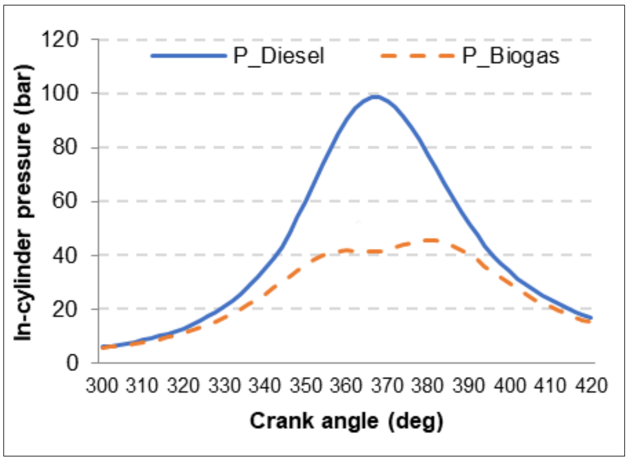

Figure 13 Comparison of in-cylinder pressure at 1600 rpm

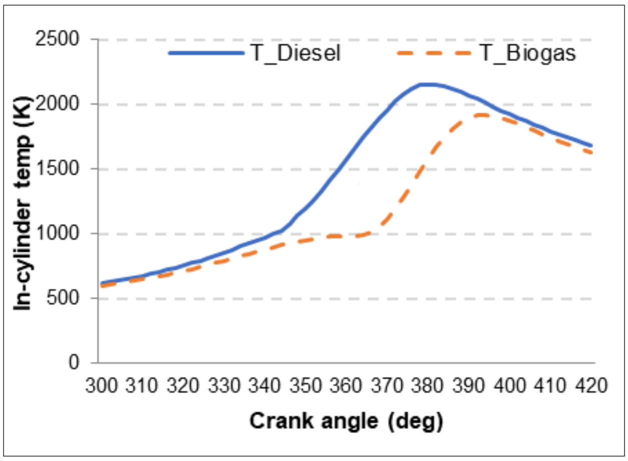

Figure 14 Comparison of in-cylinder temperature at 1600 rpm

3.5. The effect of ignition timing on biogas engine performance

To assess the effect of IT on the technical performance of the engine operating on biogas, the IT was varied from 3° to 21° before TDC, with an increment (ΔIT) of 4°. The simulation results are presented in Figures 15 to 16.

Figure 15 shows the engine torque when operating with biogas at various IT. As the IT is gradually advanced, the torque tends to increase with engine speed from 1000 rpm to 2380 rpm, and then gradually decreases as the engine speed continues to rise. The maximum torque value is observed at 1800 rpm with an IT of 13° before TDC. The main factors influencing the torque variation include volumetric efficiency, thermal efficiency, and frictional losses. When the IT is further advanced to 17° and 21°, the M_e profiles tend to decrease, with a more pronounced reduction observed in the low-speed range.

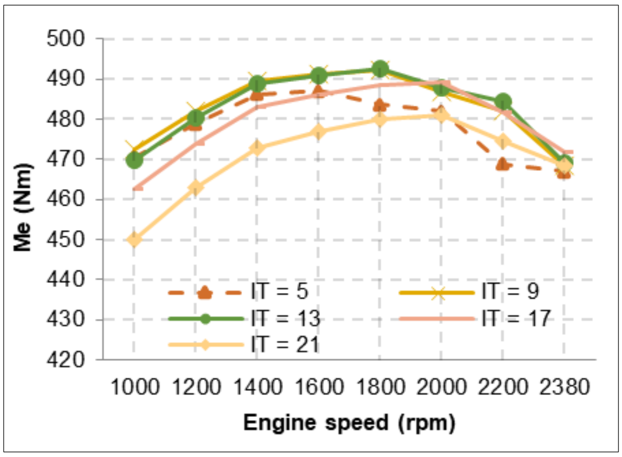

Figure 15 Comparison of brake torque pressure profiles at different IT

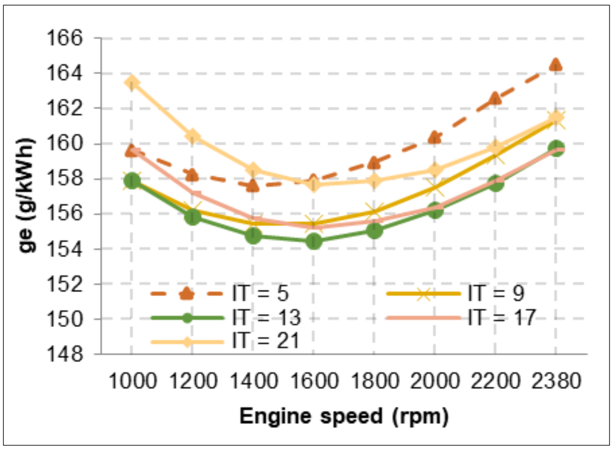

Figure 16 Comparison of ge pressure profiles at different IT

Figure 16 presents the brake specific fuel consumption (BSFC) of the biogas-fueled engine at various ITs. As the IT is progressively advanced, the BSFC tends to decrease with engine speed from 1000 rpm to 1600 rpm, and then gradually increases as engine speed continues to rise. The lowest SFC value is observed at 1600 rpm with an IT of 13° before TDC. When the IT is further advanced to 17° and 21°, the BSFC tends to increase, indicating a decline in engine efficiency.

3.6. The effect of intake temperature on biogas engine performance

The intake charge temperature is a critical parameter that influences engine operation. In this section, we assess the impact of intake air temperature on engine power at an intermediate engine speed, under varying load conditions from full load down to 70% load, corresponding to different intake temperatures of 25°C, 50°C, and 75°C.

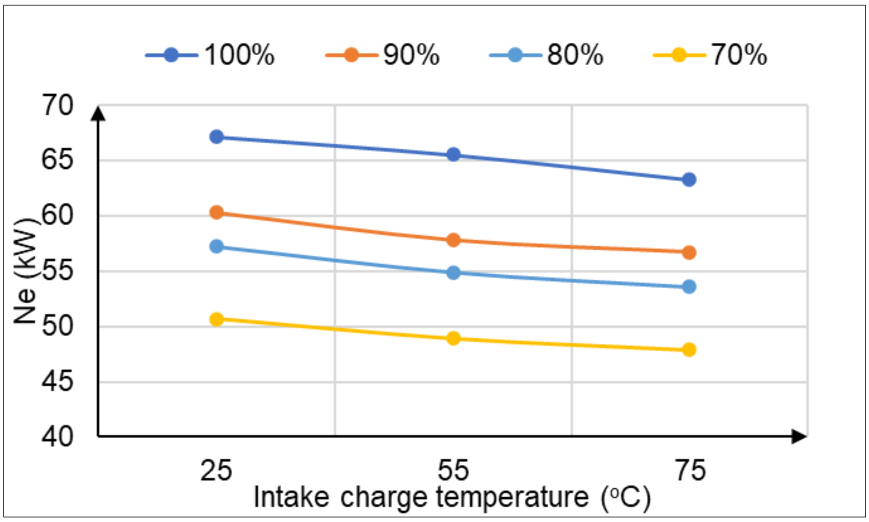

Figure 17 Comparison of brake power at different intake air temperatures

The results presented in Table 3 and Figure 17 indicate that the intake charge temperature significantly influences the engine's power output. As the ambient temperature increases from 25°C to 75°C, the power output consistently decreases across all load levels. For instance, at full load (100%), the power output drops from 67.14 to 63.28, representing a reduction of approximately 5.75%. Similarly, at 90% load, the power decreases from 60.31 to 56.69, demonstrating a steady decline in performance with rising intake temperatures.

Table 3 In-cylinder parameter at full load condition

Intake charge temperature (°C)	Peak in-cylinder temperature (K)	Peak in-cylinder pressure (bar)	Combustion starts at temperature (K)	Combustion starts at pressure (bar)	Brake power (kW)
25	1709.05	43.21	871.18	37.65	67.14
50	1709.18	42.52	872.54	36.96	65.52
75	1707.5	41.45	874.33	36.1	63.28

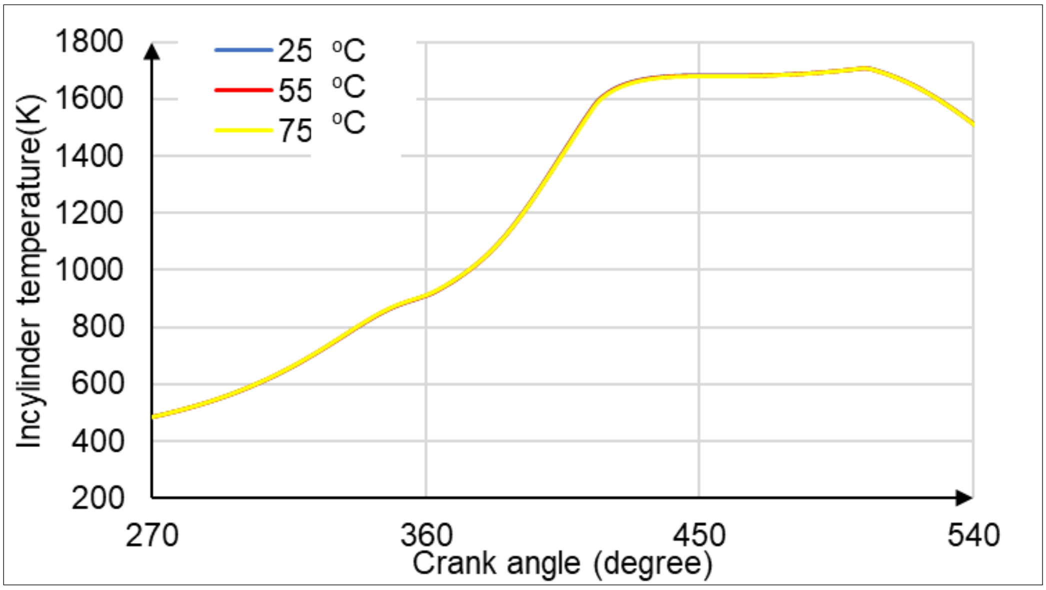

Figure 18 Comparisons of in-cylinder temperature at different intake air temperatures

Based on the data from Table 3, combined with Figures 18 and 19, it is evident that the intake charge temperature has a significant influence on the combustion process and the overall system efficiency. As the intake charge temperature increases from 25°C to 75°C, the peak combustion temperature slightly decreases from 1709K to 1707K, while the peak pressure drops from 43.21 bar to 41.45 bar. Meanwhile, the temperature at the start of combustion rises from 871K to 874K, and the pressure at the start of combustion decreases from 37.65 bar to 36.1 bar. These changes indicate that a higher intake charge temperature leads to lower peak temperature and pressure, thereby reducing combustion efficiency.

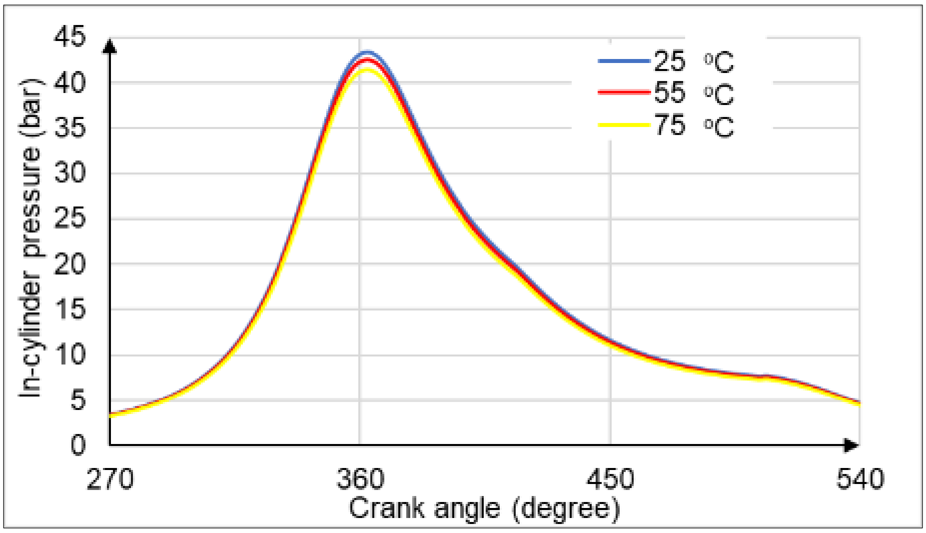

Figure 19 Comparions of in-cylinder pressure at full load,1600 rpm as the intake air temperature varied

The temperature and pressure profiles versus crank angle further illustrate this trend, showing a slight reduction in peak values at higher intake charge temperatures. This directly impacts system power output, which decreases from 67.14 kW (at 25°C) to 63.28 kW (at 75°C). These results reflect the negative effect of elevated intake charge temperatures on thermal efficiency, highlighting the importance of intake temperature control to ensure optimal performance and operational stability of the system.

Nomenclature

CO	**Carbone monoxide**
NO_x	Nitrogen oxide
HC	Hydrocarbons
CO_2	Carbone dioxide
S.I.	Spark ignition engine
LHV	Lower heating value
RON	Research octane number
A/F	Air-to-fuel ratio
IT	Ignition timing
TDC	Top dead center
BSEC	Brake-specific energy consumption
BSFC	Brake-specific fuel consumption

Abbreviations

ε_0	The compression ratios before modification
ε	The compression ratios after modification
S	The piston stroke
a	The thickness of the spacer to be added
m	Mass of fuel
N_e	Brake power
M_e	Brake torque

4. Conclusion

The simulation study of an engine operating with biogas fuel was conducted under full-throttle speed characteristic conditions using AVL Boost software. The key findings are as follows:

- On average, the specific energy consumption improved by approximately 51.48% when using biogas.
- Engine power and torque decreased by around 25% due to the displacement of intake air by the biogas volume and the slower combustion rate of biogas compared to diesel.
- Soot emissions were eliminated, while HC emissions were generated; the HC emissions amounted to about 12% of the previously existing soot emissions. CO emissions increased by 97%, whereas NO_x emissions decreased by 99%.
- For the design of the ignition system aimed at developing biogas-fueled engines, the ignition timing should be adjusted within a minimum range of 11° to 19° before TDC.
- The intake air temperature significantly affects engine performance. When evaluated at medium engine speed under moderate to high load conditions, the results indicate that the intake charge temperature should be maintained below 50°C to ensure optimal engine performance.

Compliance with ethical standards

Disclosure of conflict of interest

No conflict of interest to be disclosed.

References

[1] Nguyen, T., Pham, M., & Anh, T. L. (2020). Spray, combustion, performance and emission characteristics of a common rail diesel engine fueled by fish-oil biodiesel blends. Fuel, 269: 117108. doi:10.1016/j.fuel.2020.117108

[2] Tuan, Nguyen Thanh., & Nguyen, Phu Dong. (2022). Improving performance and reducing emissions from a gasoline and liquefied petroleum gas bi-fuel system based on a motorcycle engine fuel injection system. Energy for Sustainable Development, 67: 93-101. doi.org/10.1016/j.esd.2022.01.010.

[3] Nguyen Duc, K., Nguyen Duy, V., Hoang-Dinh, L., Nguyen Viet, T., & Le-Anh, T. (2019). Performance and emission characteristics of a port fuel injected, spark ignition engine fueled by compressed natural gas. Sustainable Energy Technologies and Assessments, 31: 383–389. doi:10.1016/j.seta.2018.12.018

[4] The, Truc Nguyen., Tran, Anh Duc., Nguyen, Cam Van., Nguyen, Khac Tung., Hoang, Dinh Long., Trinh, Xuan Phong., and Khanh, Nguyen Duc. (2022). Mechanical and Thermal Load Effect on Piston Crown of a Biogas Engine: A Simulation Approach. ASEAN Journal on Science and Technology for Development, 39 (3): 125-131. doi:10.29037/ajstd.870

[5] Karagöz, Y., Sandalcı, T., Koylu, U. O., Dalkılıç, A. S., & Wongwises, S. (2016). Effect of the use of natural gas–diesel fuel mixture on performance, emissions, and combustion characteristics of a compression ignition engine. Advances in Mechanical Engineering, 8(4). doi:10.1177/1687814016643228

[6] Xu, C.C. & Cho, H.M. (2016). The study of the effect of the natural gas in the CNG engine. International Journal of Applied Engineering Research, 11(12): 7688–7690. http://www.ripublication.com

[7] Huang, J., & Crookes, R.J. (1998). Assessment of simulated biogas as a fuel for the spark ignition engine. Fuel, 77:1793–1801. doi:10.1016/S0016-2361(98)00114-8.

[8] Hosmath, R.S.; Banapurmath, N.R.; Khandal, S.V.; Gaitonde, V.N.; Basavarajappa, Y.H.; Yaliwal, V.S. (2016). Effect of compression ratio, CNG flow rate and injection timing on the performance of dual fuel engine operated on honge oil methyl ester (HOME) and compressed natural gas (CNG). Renewable Energy, 93: 579–590. doi:10.1016/j.renene.2016.03.010

[9] Yontar, A. A., & Doğu, Y. (2018). Experimental and numerical investigation of effects of CNG and gasoline fuels on engine performance and emissions in a dual sequential spark ignition engine. Energy Sources, Part A: Recovery, Utilization, and Environmental Effects, 40(18): 2176-2192. doi:10.1080/15567036.2018.1495783

[10] Aslam, M.U., Masjuki, H.H., Kalam, M.A., Abdesselam, H., Mahlia, T.M.I., Amalina, M.A. (2006). An experimental investigation of CNG as an alternative fuel for a retrofitted gasoline vehicle. Fuel. 85:717–724. doi:10.1016/j.fuel.2005.09.004.

[11] Surata, I. W., Nindhia, T. G. T., Atmika, I. K. A., Negara, D. N. K. P., Putra, I. W. E. P. Simple Conversion Method from Gasoline to Biogas Fueled Small Engine to Powered Electric Generator. Energy Procedia 2014; 52: 626–32. https://doi.org/10.1016/j.egypro.2014.07.118

[12] Porpatham, E., Ramesh, A., Nagalingam, B. Effect of compression ratio on the performance and combustion of a biogas fuelled spark ignition engine. Fuel 2011; 95: 247-56. https://doi.org/10.1016/j.fuel.2011.10.059

[13] Barik, D., Murugan, S. Experimental investigation on the behavior of a DI diesel engine fueled with raw biogas–diesel dual fuel at different injection timing. J. Energy Inst 2016; 89(3): 373–88. https://doi.org/10.1016/j.joei.2015.03.002

[14] Converting Diesel Engines to Natural Gas, https://www.omnitekcorp.com/xyz/Omnitek%20Biogas%20Conversion.pdf; 2013 [accessed 3 June 2024].

[15] Vasan, V., Sridharan, N.V., Feroskhan, M., Vaithiyanathan, S., Subramanian, B., Tsai, P.C., Lin, Y.C., Lay, C.H., Wang, C.T., Ponnusamy, V.K. Biogas production and its utilization in internal combustion engines - A review. Process Safety and Environmental Protection 2024, 186: 518-539. https://doi.org/10.1016/j.psep.2024.04.014.

[16] Truong, N.P., Duc, K.N., Phong, T.X., Nghia, N.T. The effects of HHO-enriched air on the combustion process and emission variation of simulated-biogas fueled spark ignition engine, International Journal of Thermofluids 2025, 26: 101146. https://doi.org/10.1016/j.ijft.2025.101146.

[17] Dugala, N.S., Goindi, G.S. & Sharma, A. Experimental investigations on the performance and emissions characteristics of dual biodiesel blends on a varying compression ratio diesel engine. SN Appl. Sci. 2021, 3: 622. https://doi.org/10.1007/s42452-021-04618-0

[18] The, T.N., Tran, A.D., Nguyen, C.V., Nguyen, K.T., Hoang, D.L., Trinh, X.P., and Khanh, N.D. Mechanical and Thermal Load Effect on Piston Crown of a Biogas Engine: A Simulation Approach," ASEAN Journal on Science and Technology for Development 2022, 39(3): 4. https://doi.org/10.29037/ajstd.870

[19] Pizzuti, L., Martins, C.A., Lacava, P.T. Laminar burning velocity and flammability limits in biogas: A literature review. Renewable and Sustainable Energy Reviews 2016; 62: 856-65. https://doi.org/10.1016/j.rser.2016.05.011.

[20] Nayak, C., Sahoo, B.B. Comparative assessment of biogas and producer gas with diesel in a twin cylinder dual-fuel diesel engine. J Braz. Soc. Mech. Sci. Eng 2020; 42: 531. https://doi.org/10.1007/s40430-020-02615-9

[21] AVL. AVL Boost Combustion Model. Boost user's guide. Austria; 2011.

[22] AVL. Thermodynamic cycle simulation Boost. Version 3.2. Boost user's guide. Austria; 2011.

[23] Zhou, H., Li, X., & Liu, F. . Soot formation and oxidation mechanisms in a diesel engine separated swirl combustion system. Fuel 2019, 257: 115955. doi:10.1016/j.fuel.2019.115955

[24] Depcik, C., & Assanis, D. One-dimensional automotive catalyst modeling. Progress in Energy and Combustion Science 2005, 31(4): 308–369. doi:10.1016/j.pecs.2005.08.001